

concentrated to give hydroxycyclohexanone ethylene ketal **23** as a white solid (209 mg): mp 67–75 °C; $[\alpha]_D^{25} -15^\circ$ (*c* 0.53); IR (CCl₄) 3544, 2210 cm⁻¹; ¹H NMR δ 0.93 (s, 3 H), 3.33 (br s, 1 H), 3.95 (s, 4 H); mass spectrum (70 eV), *m/z* (relative intensity) no M⁺, 117 (5), 116 (8), 115 (100), 114 (6), 99 (4), 86 (31), 71 (10).

(2S)-2-Methyl-d₃-2-methylcyclohexanone (3). A solution of the 5-hydroxycyclohexanone ethylene ketal **23** (185 mg, 0.979 mmol) and *p*-toluenesulfonyl chloride (4.83 mg, 2.54 mmol) in pyridine (3.5 mL) was stirred at -10 °C for 18 h. The reaction mixture was poured onto ice and after 20 min the precipitate formed was isolated by filtration and dried under vacuum to give 313 mg of tosylate: ¹H NMR δ 0.82 (s, 2.25 H), 0.97 (s, 0.75 H),³² 2.43 (s, 3 H), 3.88 (s, 4 H), 4.58 (m, 1 H), 7.36 (d, 2 H, *J* = 8 Hz), 7.78 (d, 2 H, *J* = 8 Hz).

The tosylate (266 mg, 0.776 mmol) in THF (3 mL) was treated with lithium triethylborohydride (1.8 mL, 1 M in THF) and the resulting solution was heated at reflux for 24 h. To the cool reaction mixture was added 3 N sodium hydroxide (2 mL) followed by 30% hydrogen peroxide (2 mL). After the mixture was stirred for 20 min, the aqueous layer was separated and extracted with ether. The combined ethereal extract was washed with water and brine, dried, and concentrated to produce

(32) After removal of the C-5 substituent, the two separated methyl resonances merged into a singlet.

(2S)-2-methyl-d₃-2-methylcyclohexanone ethylene ketal (234 mg).

The cyclohexanone ethylene ketal (50 mg, 0.289 mmol) in ether (2 mL) was treated with 10% hydrochloric acid (0.4 mL) for 11.5 h at 25 °C. A saturated sodium carbonate solution was added and the organic layer was isolated. The organic phase was washed with brine, dried, and concentrated to give 30 mg of cyclohexanone **3**. Purification was accomplished by preparative VPC (column A, 150 °C): IR (CCl₄) 2210, 1707 cm⁻¹; mass spectrum (70 eV), *m/z* (relative intensity) 129 (M⁺, 15), 85 (100), 83 (17), 72 (38), 55 (42).

(2S)-2-Methyl-¹³C-2-methylcyclohexanone (4). The title compound **4** was synthesized from (-)-carvone by the synthetic method outlined in Scheme III except that iodomethane-¹³C (82% isotopic purity; Stohler Isotopic Chem.) was substituted for iodomethane-d₃: ¹H NMR (CCl₄) δ 1.03 (s, 1.08 H), 1.03 (d, 2.46 H, *J*(¹³C-C-C) = 5 Hz), 1.03 (d, 2.46 H, *J*(¹³C-H) = 127 Hz); mass spectrum (70 eV), *m/z* (relative intensity) 127 (M⁺, 25), 83 (100), 70 (25), 57 (21).

Acknowledgments. We acknowledge the valuable technical assistance of Ms. Ruth Records and thank Professor David Lightner (University of Nevada) for providing us with a preprint of ref 23. Partial financial support was provided by grants from the National Science Foundation (CHE 78-27413) and the National Institutes of Health (GM 20276-06).

Heterogeneous Rates of Electron Transfer. Application of Cyclic Voltammetric Techniques to Irreversible Electrochemical Processes

R. J. Klingler and J. K. Kochi*

Department of Chemistry, Indiana University, Bloomington, Indiana 47401.

Received January 14, 1980

Abstract: The anodic peak potentials in the irreversible cyclic voltammograms of various homoleptic alkylmetals in acetonitrile show a striking linear correlation with their ionization potentials *I*_D determined in the gas phase. Application of various transient electrochemical techniques proves that the electrode process arises from a totally irreversible ECE sequence in which the peak potential is determined solely by the kinetics of heterogeneous electron transfer and diffusion—uncomplicated by any follow-up chemical reaction. As a result, the anodic peak potential *E*_p can be directly related to the activation free energy for electron transfer, and the correlation of *E*_p and *I*_D represents a linear free-energy relationship. The mechanism of heterogeneous electron transfer is described as an outer-sphere process, dependent only on the driving force for one-electron oxidation and independent of steric effects of the alkylmetal. The close relationship between the activated complexes for heterogeneous and homogeneous electron transfer is emphasized in a direct comparison of the electrochemical process with the oxidation of the same alkylmetals by a series of poly(pyridine)iron(III) complexes in solution.

Introduction

Many organometals are excellent electron donors by virtue of the powerful effect exerted by alkyl groups as σ-donor ligands.¹⁻⁴ Consequently, the ionization potential of a given alkylmetal is always lower than that of most other metal derivatives.⁵ This property of alkyl ligands confers upon organometals a ubiquitous role as electron donors in a variety of electron-transfer and charge-transfer interactions with inorganic as well as organic electrophiles and oxidants.⁶

Ionization from the substitution-inert alkylmetals of the main-group elements such as Sn, Pb, Hg, etc., occurs from a

carbon-metal bonding orbital (HOMO). As a result, the structure of the alkyl ligand strongly affects the ionization potential of the alkylmetal.^{4,7} Coupled with the availability of a wide variety of alkyl ligands, the structures of alkylmetals can be finely tuned to cover a range of electron-donor and steric properties. Such a control over electronic and steric effects makes alkylmetals ideally suited for the study of electron-transfer mechanisms. Thus many alkylmetals are readily oxidized by the well-known oxidants, tris(phenanthroline)iron(III)^{8,9} and hexachloroiridate(IV),¹⁰⁻¹² by a rate-limiting electron-transfer step (e.g., see eq 1-3).

(1) Jonas, A. E.; Schweitzer, G. K.; Grimm, F. A.; Carlson, T. A. *J. Electron Spectros. Relat. Phenom.* **1972**, *1*, 29.

(2) Evans, S.; Green, J. C.; Joachim, P. J.; Orchard, A. F.; Turner, D. W.; Maier, J. P. *J. Chem. Soc., Faraday Trans. 2* **1972**, *68*, 905.

(3) Boschi, R.; Lappert, M. F.; Pedley, J. B.; Schmidt, W.; Wilkins, B. T. *J. Organomet. Chem.* **1973**, *50*, 69.

(4) Fehlner, T. P.; Ulman, J.; Nugent, W. A.; Kochi, J. K. *Inorg. Chem.* **1976**, *15*, 2544.

(5) Kochi, J. K. "Organometallic Mechanisms and Catalysis"; Academic Press: New York, 1978; Table IV, p 454, and Table I, p 501.

(6) See ref 5, Chapters 16-18.

(7) (a) Beltram, G.; Fehlner, T. P.; Mochida, K.; Kochi, J. K. *J. Electron Spectros. Relat. Phenom.* **1980**, *18*, 153. (b) Wong, C. L.; Mochida, K.; Gin, A.; Weiner, M. A.; Kochi, J. K. *J. Org. Chem.* **1979**, *44*, 3979.

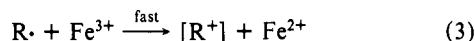
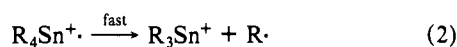
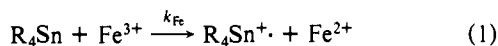
(8) Peloso, A. *J. Organomet. Chem.* **1974**, *67*, 423.

(9) Wong, C. L.; Kochi, J. K. *J. Am. Chem. Soc.* **1979**, *101*, 5593.

(10) (a) Abley, P.; Dockal, E. R.; Halpern, J. *J. Am. Chem. Soc.* **1972**, *94*, 659. (b) Anderson, S. N.; Ballard, D. H.; Chrzastowski, J. Z.; Dodd, D.; Johnson, M. D. *J. Chem. Soc., Chem. Commun.* **1972**, 685.

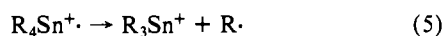
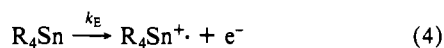
(11) (a) Chen, J. Y.; Gardner, H. C.; Kochi, J. K. *J. Am. Chem. Soc.* **1976**, *98*, 6150. (b) Gardner, H. C.; Kochi, J. K. *J. Am. Chem. Soc.* **1975**, *97*, 1855.

(12) Chen, J. Y.; Kochi, J. K. *J. Am. Chem. Soc.* **1977**, *99*, 1450.



The rate constant k_{Fe} for electron transfer to iron(III) in eq 1 follows the Marcus correlation¹³ with a predicted Brønsted slope $\alpha = 0.5$ for an outer-sphere mechanism.⁹ As expected for an outer-sphere process, the linear free-energy relationship is not subject to steric effects of the alkylmetal since even the highly hindered *tert*-butyl and neopentyl derivatives are included in the correlation. On the other hand, electron transfer to iridate(IV) shows deviations which vary with the steric hindrance of the alkylmetal.⁹ Indeed such steric effects can be exploited in the differentiation of outer-sphere from inner-sphere mechanisms for electron transfer.¹⁴

We now apply the same steric probe to the corresponding electrochemical process, for which the analogous mechanism for heterogeneous electron transfer is represented by an ECE sequence as shown in eq 4–6.



Our initial problem is to relate the rate constant k_E for the heterogeneous electron-transfer step in eq 4 to the anodic peak potential E_p of the cyclic voltammogram by showing that the electrochemical process is totally irreversible. Under these conditions, the charge-transfer process is intrinsically slow, and the kinetic control of the electrochemical reaction is not significantly affected by the follow-up reactions.¹⁵ The rates and activation parameters for electron transfer obtained in this manner for the heterogeneous (electrode) process can then be compared to the corresponding values for the homogeneous process examined earlier⁹ with a series of poly(pyridine) complexes of iron(III) in the same medium.

Results and Discussion

The homoleptic alkylmetals employed in this study consisted of the tetraalkyl derivatives of the group 4 elements, silicon, germanium, tin, and lead, as well as the two-coordinate dialkylmercury compounds. The ionization potentials I_D of the alkylmetals are available from previous measurements.^{4,7,9}

I. Cyclic Voltammetry (CV) of Homoleptic Alkylmetals. The single-sweep cyclic voltammograms of the various alkylmetals listed in Table I were recorded with a stationary platinum microelectrode in acetonitrile solutions at 25 °C. The cyclic voltammograms of these compounds are all characterized by an anodic wave showing a well-defined current maximum but no cathodic wave on the reverse scan even at sweep rates up to 10 V s⁻¹ and temperatures as low as -35 °C. The details of the sweep dependence of the anodic wave are shown in Figure 1 for tetraethyltin as a representative alkylmetal. A closer inspection of the cyclic voltammograms reveals that the current in the foot of the anodic wave is singularly independent of the sweep rate. Such a behavior, originally noted by Reinmuth,¹⁸ strongly suggests that electron transfer from these alkylmetals is electrochemically unidirectional, i.e., totally irreversible. We shall apply a number of more rigorous

Table I. Cyclic Voltammetric Data for Homoleptic Alkylmetals^a

compd	E_p, V^b	$E_p - E_{p/2}, mV^b$	$i_p/Cv^{1/2} c$	I_D, eV^d
Et ₄ Si	2.56	130	0.026	9.78
Me ₄ Ge	2.64	170	0.018	10.02
Et ₄ Ge	2.24	170	0.015	9.41
Me ₄ Sn	2.48	140	0.021	9.69
Et ₄ Sn	1.76	130	0.027	8.93
EtSnMe ₃	1.96	170	0.024	9.10
<i>s</i> -Bu ₄ Sn	1.45	150	0.022	8.45
<i>i</i> -Bu ₄ Sn	1.77	130	0.023	8.68
<i>n</i> -Bu ₄ Sn	1.75	140	0.021	8.76
<i>i</i> -Pr ₄ Sn	1.51	130	0.026	8.46
neopentyl ₄ Sn	1.80	150	0.027	8.67
<i>t</i> -Bu ₂ SnMe ₂	1.25	140	0.022	8.22
Me ₄ Pb	1.80	180	0.012	8.90
Et ₄ Pb	1.26	160	0.014	8.13
Et ₂ PbMe ₂	1.56	180	0.016	8.45
<i>n</i> -Pr ₂ Hg	1.39	180	0.025	8.29
EtHgMe	1.70	170	0.022	8.84

^a Measured with a stationary platinum microelectrode at 20 mV s⁻¹ in acetonitrile containing tetraethylammonium perchlorate as supporting electrolyte at 25 °C. ^b Potential relative to saturated NaCl-SCE. ^c In units of A M⁻¹ (s/mV)^{1/2}. ^d Data from ref 7 and 9.

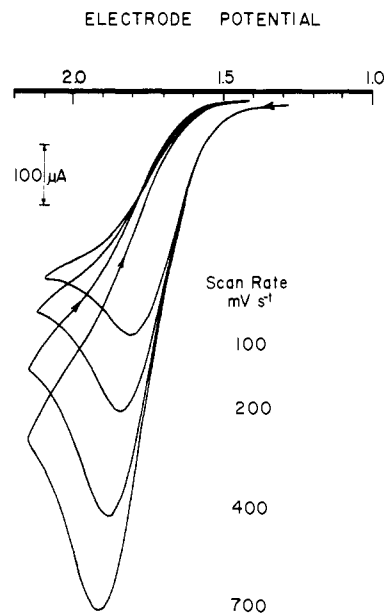


Figure 1. First-scan cyclic voltammograms of 7×10^{-3} M tetraethyltin in acetonitrile solution containing 0.1 M TEAP at a platinum microelectrode using various sweep rates. Electrode potentials in volts vs. saturated NaCl-SCE.

electrochemical criteria to establish the totally irreversible nature of the anodic oxidation of alkylmetals (vide infra), but suffice it to mention here that the absence of the reverse electron-transfer step indicates that the oxidized alkylmetal cation is highly unstable. Indeed, independent measurements employing double potential step chronoamperometry¹⁹ establish the lifetime of this species to be less than 1 ms (see Experimental Section).

Although the general appearance of the anodic wave remains relatively unchanged with various alkylmetals, the peak potentials E_p are subject to large and systematic variations, in accord with the ionization potentials, as shown in Figure 2. Thus the breadths of the waves measured at the half-widths (listed as $E_p - E_{p/2}$ in the third column of Table I) remain relatively constant at ~ 150 mV, which is considerably larger than the 59 mV expected for a reversible charge-transfer step.²⁰ The anodic peak potentials

(13) Marcus, R. J.; Zwolinski, B. J.; Eyring, H. *J. Phys. Chem.* **1954**, *58*, 432. Marcus, R. A. *J. Chem. Phys.* **1956**, *24*, 966. *Ibid.* **1957**, *26*, 867. *Discuss. Faraday Soc.* **1960**, *29*, 21. For a recent summary see: Sutin, N. *Inorg. Biochem.* **1973**, *2*, 611.

(14) Fukuzumi, S.; Wong, C. L.; Kochi, J. K. *J. Am. Chem. Soc.*, in press.

(15) For the variation in the peak potential in linear-sweep voltammetry of totally irreversible systems, see ref 16 and 17.

(16) Nadjo, L.; Savéant, J. M. *Electroanal. Chem.* **1973**, *48*, 113.

(17) Compare also the original theory by Delahey, P. "New Instrumental Methods in Electrochemistry"; Interscience: New York, 1954; pp 83–86.

(18) Reinmuth, W. H. *Anal. Chem.* **1960**, *32*, 1891.

(19) Hanafey, M. K.; Scott, R. L.; Ridgway, T. H.; Reilly, C. N. *Anal. Chem.* **1978**, *50*, 116.

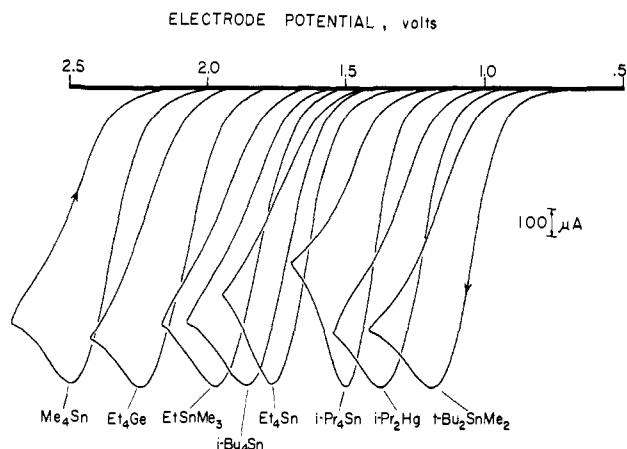


Figure 2. Single-scan cyclic voltammograms of some representative alkylmetals in acetonitrile solutions, showing the variation of the anodic peak potentials with structure.

Table II. Diffusion Coefficients and Coulometric n Values for Alkylmetals^a

diffusion coefficient		coulometry		
alkylmetal ^b	$10^5 D$, cm ² s ⁻¹	alkylmetal ^c	E , V ^d	n ^e
	<i>i</i> -Pr ₄ Sn			
<i>n</i> -Bu ₄ Sn	1.7	<i>i</i> -Pr ₄ Sn	1.5	2.09 ± 0.05
<i>i</i> -Bu ₄ Sn	1.9	<i>n</i> -Bu ₄ Sn	1.8	1.91 ± 0.05
Et ₄ Sn	1.8	<i>t</i> -Bu ₂ SnMe ₂	1.5	1.83 ± 0.05

^a In acetonitrile solutions at 25 °C with 0.1 M tetraethylammonium perchlorate as supporting electrolyte. ^b 10⁻² M. ^c 10⁻³ to 10⁻⁴ M. ^d Versus saturated NaCl-SCE. ^e Number of electrons passed per alkylmetal.

are reproducible to within ±50 mV. No aging of the electrode was apparent on a week to week basis, suggesting that the surface activity of the platinum is not a critical factor with these alkylmetals. Furthermore, there are no complications on the electrodes arising from the deposition of alkylmetal products of oxidation, since the response does not deteriorate upon continued electrolysis of the same solution for prolonged periods.²¹

The anodic peak current i_p in the cyclic voltammogram is proportional to the square root of the sweep rate v (compare Figure 1), as well as the concentration C of the alkylmetal in the range 5×10^{-2} to 5×10^{-4} M, both of which are consistent with diffusion as the rate-limiting step.²⁰

In this series of related alkylmetals, the near constancy of the current function $i_p/Cv^{1/2}$ in column 4 of Table I indicates that the diffusion coefficients are rather insensitive to structure. Indeed, in Table II an independent measurement of the diffusion coefficients of a select number of alkylmetals relative to a ferrocene standard bears out this conclusion.

Coulometric measurements were carried out at a constant potential corresponding to the CV peak potential of the alkylmetal. The bulk electrolysis of a 10⁻² M solution at a platinum gauze electrode afforded 2 electrons per alkylmetal, which is in excellent accord with eq 4–6 and the chemical stoichiometry described previously.^{9,11}

II. Correlation of Ionization Potentials I_D of Alkylmetals with Anodic Peak Potentials E_p . The anodic peak potentials in Table I are shown to be linearly related to the ionization potentials in Figure 3. This remarkable correlation extends over a 2-V range in potentials, and it includes both the four-coordinate tetraalkylmetals of silicon, germanium, tin, and lead as well as the

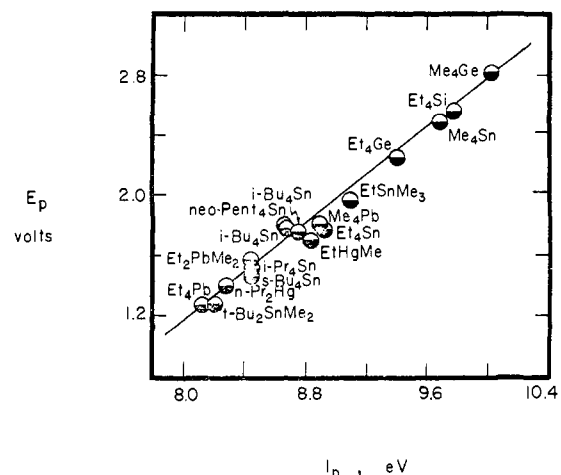


Figure 3. Linear correlation of anodic peak potentials E_p in acetonitrile solution and ionization potentials I_D of various alkylmetals in the gas phase.

two-coordinate dialkylmercurials. A most important feature of the linear correlation in Figure 3 is the striking insensitivity to steric effects, despite large changes in the structures of the alkyl ligands. In particular, increasing the branching of the alkyl ligand at the β carbon with methyl groups in the homologous series CH_3CH_2 , $\text{CH}_3\text{CH}_2\text{CH}_2$, $(\text{CH}_3)_2\text{CHCH}_2$, and $(\text{CH}_3)_3\text{CCH}_2$ leads to minimal deviations from the correlation line. Thus even the highly sterically hindered tetra-n-pentyltin²² is included precisely in the correlations with the other tetraalkylmetal and dialkylmercury compounds. The same applies to α branching in the series: CH_3 , CH_3CH_2 , $(\text{CH}_3)_2\text{CH}$, and $(\text{CH}_3)_3\text{C}$. Tetra-*tert*-butyltin unfortunately is unknown, but the most hindered *tert*-butyl derivative we had available, *t*-Bu₂SnMe₂, is nicely included with the other alkylmetals in the linear correlation expressed in eq 7.

$$E_p = 0.76I_D + \text{constant} \quad (7)$$

The absence of steric effects on the correlation of the anodic peak potential E_p with the gas-phase ionization potential I_D reflects the outer-sphere mechanism for electron transfer in the anodic oxidation of alkylmetals.⁹ Indeed, we show in the following treatment that the linear correlation in Figure 3 for various alkylmetals derives from values of E_p which are directly related to the activation free energies for heterogeneous electron transfer. The analysis depends on the interpretation of the peak potential, particularly the significance of E_p for the anodic waves in Table I. Indeed, electrochemical theory is well-developed for the analysis of the shifts in peak potentials (with such variables as scan rate, concentration, etc.) to yield quantitative information about the nature and magnitude of the chemical reactions following electron transfer.^{20,24,25} However, the converse is not true, and it is possible for E_p to be independent of the rates of the chemical reactions following electron transfer. Such a situation can arise when the following chemical reactions are faster than the reverse electron-transfer step²⁶—such an electrochemical process is described as *totally irreversible*.²⁸

(22) Zimmer, H.; Hechenbleikner, I.; Homberg, O. A.; Danzik, M. *J. Org. Chem.* **1964**, *29*, 2632. See also: Reichle, W. T. *Inorg. Chem.* **1966**, *5*, 87.

(23) The relative sizes of alkyl ligands are related to their Taft E_s parameters, which increase for α branching in the order: Me < Et < *i*-Pr < *t*-Bu, quantitatively, as: 0, 0.07, 0.47, and 1.54, and for β branching in the order: Et < *n*-Pr < *i*-Bu < neopentyl as: 0.07, 0.36, 0.93, and 1.74 (Taft, R. W., Jr. In "Steric Effects in Organic Chemistry"; Newman, M. S., Ed.; Wiley: New York, 1956).

(24) Pletcher, D. *Chem. Soc. Rev.* **1975**, *4*, 471.

(25) (a) Streitwieser, A. In "Physical Methods of Chemistry"; Weissberger, A.; Rossiter, B. W., Eds.; Wiley-Interscience: New York, 1971. (b) Saveant, J. M.; Vianello, E. *C. R. Hebd. Seances Acad. Sci.* **1963**, *256*, 2597.

(26) We have employed a well-behaved organometallic system²⁷ to illustrate this important point, as described in the Experimental Section.

(27) Pickett, C. J.; Pletcher, D. *J. Chem. Soc., Dalton Trans.* **1975**, 879. *Ibid.* **1976**, 636.

(28) For example, see: McDonald, D. D. "Transient Techniques in Electrochemistry"; Plenum Press: New York, 1977; p 201ff.

(20) Nicholson, R. S.; Shain, I. *Anal. Chem.* **1964**, *36*, 706.

(21) This situation does not always prevail in the anodic oxidation of organometallic compounds. For example, for problems encountered with the analogous trialkylmetal hydrides, see: Klingler, R. J.; Mochida, K.; Kochi, J. K. *J. Am. Chem. Soc.* **1979**, *101*, 6626.

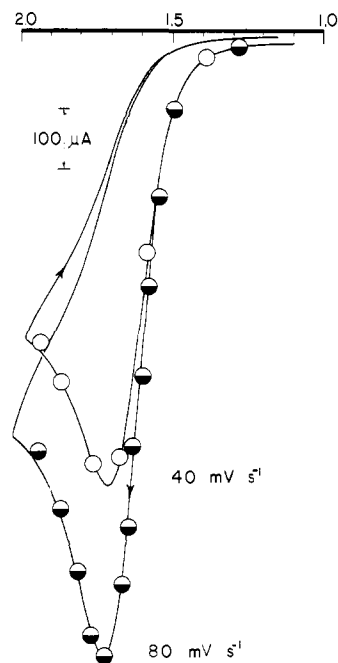
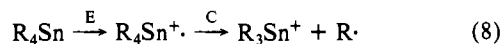


Figure 4. Calculated and experimental cyclic voltammogram for Et_4Sn in acetonitrile solution containing 0.1 M TEAP at a platinum microelectrode using scan rates of (O) 40 and (●) 80 mV s^{-1} . The calculated points are based on eq 20, using $\beta = 0.34$ and $E = E^0 + (RT/2\beta\mathcal{F}) \ln(\pi D/k_s) = 1.660$ V vs. saturated NaCl-SCE.

Total Irreversibility in Anodic Oxidation of Alkylmetals. The anodic oxidation of alkylmetals in eq 4–6 is an EC process (see eq 8). The first indication that the heterogeneous electron transfer



from alkylmetals is totally irreversible was readily apparent in the current independences of the sweep rates described in Figure 1 (vide infra).^{18,29,30} In order to establish total irreversibility in this system, we have employed additional analytical criteria based on the general expression for the rate constant for heterogeneous electron transfer in eq 9,³¹ where E is the electrode potential, β

$$k(E) = k_s \exp \left[\frac{\beta n_b \mathcal{F}}{RT} (E - E^0) \right] \quad (9)$$

is the transfer coefficient for the electrode process, n_b is the number of electrons transferred in the rate-limiting step, and E^0 is the standard potential which fixes the value of k_s ; the other notations are conventional. The application of eq 9 together with Fick's laws of diffusion leads to quantitative tests for total irreversibility based on (1) the dependence of E_p and $E_{p/2}$ on the CV sweep rate, (2) the consistency of the transfer coefficients evaluated from various properties of the CV wave, and (3) the shape of the anodic wave. Indeed the anodic oxidation of alkylmetals satisfies all of these electrochemical criteria for total irreversibility. Since these bear critical importance to the next section, the details of this analysis are included separately in the Experimental Section. We now proceed to the measurements of the heterogeneous rates of electron transfer from the CV data.

III. Rates of Heterogeneous Electron Transfer. Relationship between Anodic Peak Potentials and Ionization Potentials of Alkylmetals. Electron transfer is the rate-determining step in the anodic oxidation of alkylmetals in Table I, as witnessed by the total irreversibility of the cyclic voltammetric wave. Therefore,

(29) In contrast, for a reversible electron transfer, the current should increase with the square root of the sweep rate.^{18,20}

(30) In polarographic studies, the current dependence on the mercury drop rate (instead of the CV sweep rate) has been similarly noted. (See ref 17, p 78, for the properties of totally irreversible waves.)

(31) For reviews see: Bauer, H. H. *Electroanal. Chem.* 1968, 16, 419. Tanaka, N.; Tamamushi, R. *Electrochim. Acta* 1964, 9, 963.

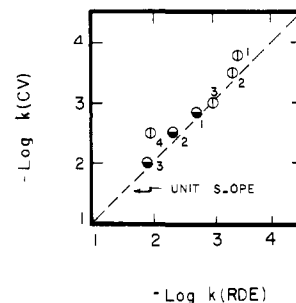


Figure 5. Agreement between the heterogeneous rate constants for (●) Et_4Pb and (○) $s\text{-Bu}_4\text{Sn}$ obtained by CV, using eq 11, and those obtained for the rotated-disk electrode (RDE), using eq 21, at $E = 1.155$ (1), 1.220 (2), 1.317 (3), and 1.411 (4) V vs. saturated NaCl-SCE, shown by the fit to the line drawn with unit slope.

the observed anodic current can be interpreted solely in terms of the expression for the potential dependence of the rate constant for electron transfer in eq 9 together with Fick's laws of diffusion,³² without reference to the nature of the fast follow-up chemical reactions such as those in eq 5 and 6. On this basis, we have carried out the analysis of the CV wave by using the method of Nicholson and Shain.²⁰ The results of these calculations are indicated by the circles in Figure 4, which clearly show excellent agreement with the observed currents. By the same method of calculation, Nicholson and Shain have also concluded that the rate constant $k(E_p)$ for electron transfer at the CV peak potential is given by eq 10. Combination of eq 10 and the general ex-

$$k(E_p) = 2.18 \left[\frac{D\beta n_b \mathcal{F} v}{RT} \right]^{1/2} \quad (10)$$

pression in eq 9 with $n_b = 1$ yields eq 11, in which the potential

$$k(E) = 2.18 \left[\frac{D\beta \mathcal{F} v}{RT} \right]^{1/2} \exp \left[\frac{\beta \mathcal{F}}{RT} (E - E_p) \right] \quad (11)$$

dependence of the rate constant $k(E)$ for electron transfer is expressed in terms of the CV parameters E_p and β . The validity of the method is shown in Figure 5 by the fit to the line of unit slope which relates the rate constants at various potentials calculated from eq 11 with those obtained from independent measurements using the rotated disk electrode.³³

The potential dependence of the rate constant in eq 11 may now be used to develop an understanding of the empirical correlation between E_p and I_D in Figure 3.³⁴ Thus, the relationship between the electrochemical rate constant and the activation free energy for electron transfer is given by eq 12,³⁵ where the elec-

$$\Delta G^*(E) = -RT \ln \frac{k(E)}{Z} \quad (12)$$

trochemical frequency factor Z is also expressed in units of cm s^{-1} . The relationship between the peak potential and the activation free energy is obtained by substituting eq 11 into eq 12 to give eq 13.

$$\Delta G^*(E) = \beta \mathcal{F} E_p - RT \left[0.780 + \frac{1}{2} \ln \left(\frac{D\beta \mathcal{F} v}{RT} \right) + \frac{\beta \mathcal{F} E}{RT} - \ln Z \right] \quad (13)$$

(32) Originally derived by Delahey (*J. Am. Chem. Soc.* 1953, 75, 1190).

(33) (a) The rate constants at various potentials calculated from eq 11 are listed in the Experimental Section in column 3 of Table VI for tetraethyllead and tetra-*n*-butyltin. (b) Note that eq 11 may only be applied over a range in which β has been shown to be a constant.

(34) (a) Since the diffusion coefficients as well as the transfer coefficients are relatively constant for this group of alkylmetals, eq 12 predicts the rate constants to be the same at the observed peak currents. Therefore, Figure 3 represents the linear relationship between the applied potential necessary to equalize the rate constant and the gas-phase ionization potentials. (b) The contribution from the transfer coefficient to eq 10 is minor. For example, the contribution of $\beta = 0.5$ to $\log k(E_p)$ is only 6% of the total amount when $D = 2 \times 10^{-5} \text{ cm}^2 \text{ s}^{-1}$ and $v = 10 \text{ mV s}^{-1}$.

(35) Marcus, R. A. *J. Phys. Chem.* 1963, 67, 853.

Table III. Cyclic Voltammetry of Iron(III) Complexes in Acetonitrile

FeL ₃ (ClO ₄) ₃ , L	E ⁰ , V ^a	i _p ^c / i _p ^{a,b}	Δ _v , mV ^c
4,7-diphenyl-1,10-phenanthroline	0.919	1.01	65
2,2'-bipyridine	0.976	1.02	70
1,10-phenanthroline	0.984	1.00	68
5-chloro-1,10-phenanthroline	1.081	1.01	67
5-nitro-1,10-phenanthroline	1.181	1.02	72

^a Versus saturated NaCl-SCE. ^b Ratio of the cathodic and anodic waves. ^c Separation of the anodic and cathodic peaks at 50 mV s⁻¹ scan rate.

At a given potential (*E*), the term within the brackets will be a constant for a series of alkylmetals in Table I, owing to the constancy of *D* and β in Table II. Thus the relationship reduces to eq 14.

$$\Delta G^*(E) = \beta \mathcal{F} E_p + \text{constant} \quad (14)$$

On the basis of eq 7 and 14, Figure 3 represents a linear free-energy relationship which correlates the activation free energy for heterogeneous electron transfer with the gas-phase ionization potentials of the alkylmetals, i.e., eq 15 or eq 16. We take the

$$\Delta G^*(E) = 0.23 I_D + \text{constant} \quad (15)$$

$$\Delta G^*(E) \propto I_D + \text{constant} \quad (16)$$

absence of steric effects in Figure 3 as an indication that the heterogeneous electron transfer to a platinum electrode proceeds via an outer-sphere mechanism, completely analogous to the homogeneous electron transfer recently established with poly(pyridine)iron(III) oxidants.⁹ These two systems are compared in greater detail in the following section.

IV. Comparison of Rates of Heterogeneous and Homogeneous Electron Transfer. The availability of a variety of substituted phenanthrolines allows a systematic variation in the standard reduction potentials for the related series of iron(III) complexes listed in Table III. The cyclic voltammetry of these iron(III) oxidants is reversible in acetonitrile solutions.

The second-order rate constants *k*_{Fe} in eq 1 for the homogeneous electron transfer from various alkylmetals to these iron(III) complexes are retabulated in Table IV for convenience. The rate constants *k*_E for heterogeneous electron transfer from the same alkylmetals at the potentials corresponding to *E*⁰ for the iron(III) complexes in Table III were calculated from eq 11, using the data in Table I. The logarithms of the heterogeneous rate constants were corrected by an amount log (*Z*_{Fe}/*Z*_E = 7.30)^{36,37} to allow direct comparison with the homogeneous data. The excellent linearity in the correlation between the homogeneous and heterogeneous rate constants is shown in Figure 6. The dashed line is drawn with a unit slope passing through the origin. Moreover, the slope of the experimental points is close to the unit slope expected, if the transfer coefficients for both the homogeneous and heterogeneous processes were the same.³⁸ The excellent agreement shown in Figure 6 between the heterogeneous and homogeneous rate constants, together with the absence of specific steric effects, provides compelling proof that the electrochemical oxidations of alkylmetals proceed by an outer-sphere electron-transfer mechanism.³⁹

(36) The electrochemical collision frequency *Z*_E was calculated from *Z*_E = (*RT*/2π*M*) where *M* is the molecular mass.³⁷ An average mass of *M* = 250 was used to obtain *Z*_E = 4.0 × 10³ cm² s⁻¹. The value of *Z*_{Fe} = 1.0 × 10¹¹ M⁻¹ s⁻¹ was used for the second-order rate constant for iron(III) oxidation. (Cf.: Moore, W. J. "Physical Chemistry", 3rd ed.; Prentice-Hall: Englewood Cliffs, NJ, 1962; Chapter 8).

(37) Saveant, J. M.; Tessier, D. *J. Phys. Chem.* **1977**, *81*, 2192.

(38) A detailed study of the potential dependence of the transfer coefficients will be presented separately. In particular, the observed slope of 0.74 in Figure 6 will be discussed in terms of the full quadratic form of the Marcus equation.

(39) (a) For a discussion of other criteria to distinguish outer-sphere and inner-sphere electrochemical steps see: Kravtsov, V. I. *J. Electroanal. Chem.* **1976**, *69*, 125. (b) For a detailed discussion of steric effects as a criterion for outer-sphere mechanisms see ref 14.

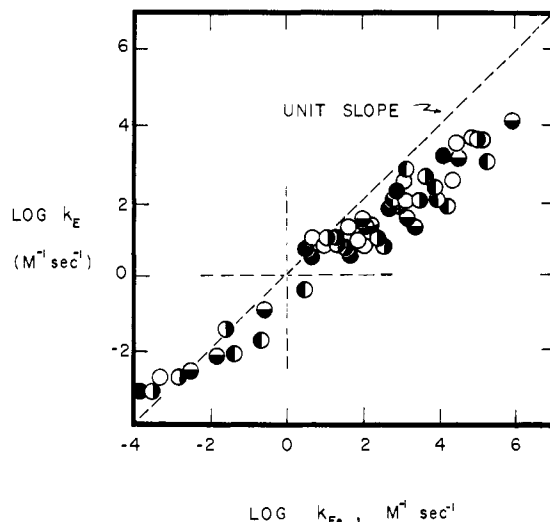


Figure 6. Correlation of the homogeneous rate constant *k*_{Fe} and the heterogeneous rate constant *k*_E from the data in Table IV at various potentials: (●) 0.919, (○) 0.976, (◐) 0.984, (◑) 1.081, and (◒) 1.181 V vs. saturated NaCl-SCE.

The striking correlation in Figure 6 also underscores the general utility of the electrochemical technique for obtaining electron-transfer rate constants over a wide range by a straightforward application of cyclic voltammetry. This simple methodology contrasts with the variety of techniques required for the measurements of the homogeneous rate constants for iron(III)⁹—spanning the inextensible range from the very slow rates to the upper limits of stopped-flow spectrophotometry.

Summary and Conclusions

The cyclic voltammograms of the homoleptic alkylmetals in Figures 1 and 2 are due to the totally irreversible ECE electrochemical process in eq 4–6. As such, the anodic peak potentials *E*_p in Table I are shown to be directly related to the activation free energies for heterogeneous electron transfer. The correlation of *E*_p and *I*_D in Figure 3 thus represents a linear free-energy relationship in which the mechanism of the heterogeneous electron transfer from alkylmetals is described as an outer-sphere process, dependent only on the driving force for one-electron oxidation. The absence of steric effects in heterogeneous electron transfer accords in Figure 6 with the outer-sphere mechanism previously established for the homogeneous rates of electron transfer to a series of poly(pyridine)iron(III) complexes in the same medium.

While a cursory expedition into the electrochemical literature might suggest that similar correlations are quite common,^{40–45} a closer examination will reveal that the majority of these cases

(40) Anodic waves vs. *I*_D⁴¹ and other thermodynamic parameters.⁴² For general discussion of the mechanism, see: (a) Ebersson, L. In "Organic Electrochemistry"; Baizer, M., Ed.; Marcel Dekker: New York, 1973; p 447. (b) Adams, R. N. "Electrochemistry at Solid Electrodes"; Marcel Dekker: New York, 1969.

(41) (a) Loveland, J. W.; Dimelar, G. R. *Anal. Chem.* **1961**, *33*, 1196. (b) Gleicher, G. J.; Gleicher, M. K. *J. Phys. Chem.* **1967**, *71*, 3693. (c) Lagutskaya, L. I.; Beilis, Yu. I. *Theor. Exp. Chem. (Engl. Transl.)* **1970**, 456. (d) Miller, L. L.; Nordblom, G. D.; Mayeda, E. A. *J. Org. Chem.* **1972**, *37*, 917. (e) Dewar, M. J. S.; Hashmall, J. A.; Trinajstić, N. *J. Am. Chem. Soc.* **1970**, *92*, 5555. (f) Nelsen, S. F.; Peacock, V.; Weisman, G. R. *Ibid.* **1976**, *98*, 5269. (g) See also ref 31 and 24.

(42) (a) Lund, H. *Acta Chem. Scand.* **1957**, *11*, 1323. (b) Neikam, W. C.; Desmond, M. M. *J. Am. Chem. Soc.* **1964**, *86*, 4811. (c) Zweig, A.; Hodgson, W. G.; Jura, W. H. *J. Am. Chem. Soc.* **1964**, *86*, 4125. (d) Zweig, A.; Lancaster, J. E.; Neglia, M. T.; Jura, W. H. *J. Am. Chem. Soc.* **1964**, *86*, 4130. (e) Zahradnik, R.; Párkányi, V. *Talanta* **1965**, *12*, 1289.

(43) For cathodic waves vs. thermodynamic parameters, see: (a) Hořtink, G. *J. Recl. Trav. Chim. Pays-Bas.* **1955**, *74*, 1525; **1958**, *77*, 555. (b) Lagutskaya, L. I.; Dadali, V. A. *Org. React. (NY, Engl. Transl.)* **1967**, *4*, 241. (c) See ref 45 for a general discussion and additional examples.

(44) (a) Pysh, E. S.; Yang, N. C. *J. Am. Chem. Soc.* **1963**, *85*, 2125. (b) Neikam, W. C.; Dimelar, G. R.; Desmond, M. M. *J. Electrochem. Soc.* **1964**, *111*, 1190.

(45) Peover, M. E. *Electroanal. Chem.* **1967**, *2*, 1.

Table IV. Comparison of the Homogeneous and Heterogeneous Rate Constants for Electron Transfer from Alkylmetals

alkylmetal	electron-transfer rate constants ^b (log k , M ⁻¹ s ⁻¹)									
	$E^a = 0.919$		$E = 0.976$		$E = 0.984$		$E = 1.081$		$E = 1.181$	
	k_E	k_{Fe}	k_E	k_{Fe}	k_E	k_{Fe}	k_E	k_{Fe}	k_E	k_{Fe}
Et ₄ Si					-3.05	-3.49	-2.55	-2.45	-2.05	-1.31
Et ₄ Ge					-1.42	-1.55	-0.93	-0.51	-0.42	-0.56
Me ₄ Sn	-2.97	-3.78	-2.68	-3.29	-2.64	-2.81	-2.15	-1.76	-1.64	-0.59
Et ₄ Sn	0.69	0.54	0.98	0.71	1.02	1.12	1.51	2.00	2.02	2.89
<i>s</i> -Bu ₄ Sn	2.26	2.94	2.55	3.06	2.59	3.65	3.09	4.55	3.59	5.21
<i>i</i> -Bu ₄ Sn	0.64	1.63	0.93	1.90	0.97	2.41	1.46	3.20	1.97	3.96
neopentyl ₄ Sn	0.48	1.72	0.77	2.04	0.81	2.55	1.31	3.42	1.81	4.25
<i>t</i> -Bu ₂ SnMe ₂					3.61	4.89				
Me ₄ Pb	0.48	0.70	0.77	0.96	0.81	1.41	1.31	2.22	1.82	3.17
Et ₄ Pb	3.23	4.07	3.52	4.50	3.56	5.03	4.05	5.97		
Et ₂ PbMe ₂	1.70	2.75	1.99	3.15	2.03	3.55	2.53	4.44	3.03	5.29
EtHgMe	0.99	1.30	1.28	1.64	1.32	2.06	1.82	3.04	2.32	3.87

^a Standard reduction potentials of $\text{R}^+\text{eL}_3^{3+}$ in Table III. Potential in volts vs. saturated NaCl-SCE. ^b Electrochemical rate constant k_E from eq 11 after correction by $\log(Z_{Fe}/Z_E) = 7.30$. Homogeneous rate constant k_{Fe} from ref 9.

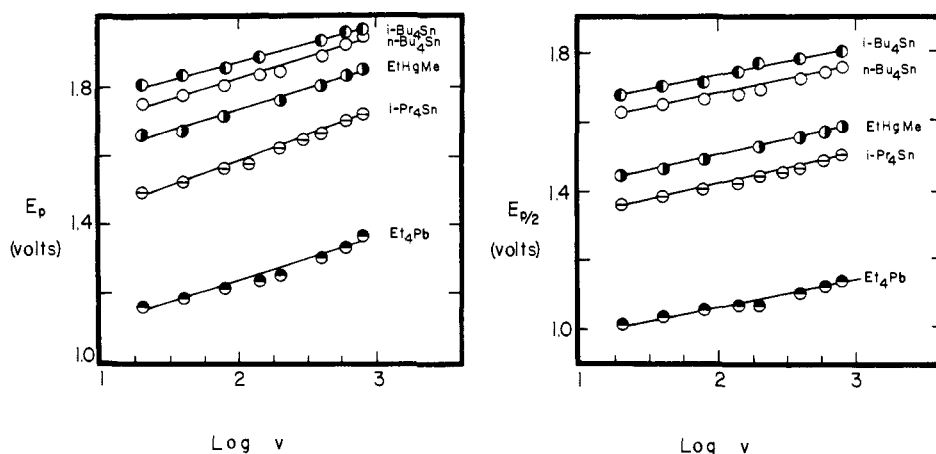


Figure 7. Variation of anodic peak potential E_p with CV sweep rate v at a platinum microelectrode at 25 °C in acetonitrile solutions containing (●) 0.1 M TEAP and 0.0084 M *i*-Bu₄Sn, (○) 0.0101 M *n*-Bu₄Sn, (◐) 0.0073 M EtHgMe, (◑) 0.0150 M *i*-Pr₄Sn, and (◒) 0.0160 M Et₄Pb.

involve an electron-transfer step which is reversible. This type of linear correlation can be interpreted as examples in which the solvation energies are approximately constant for a homologous group of compounds.⁴⁶ The existence of other linear correlations for apparently irreversible systems,⁴⁷⁻⁵¹ however, suggests that the type of analysis carried out in this study may be more generally applicable. Its success would provide a useful extrathermodynamic basis for electron-transfer processes, particularly for labile systems in which the standard reduction potentials cannot be measured directly.

Experimental Section

Materials. Preparations of the alkylmetals used in this study were described previously.⁹ Chromium hexacarbonyl was obtained from Pressure Chemical Co. and resublimed three times before use. Reagent-grade acetonitrile was further purified by refluxing it over calcium hydride, then treating it with potassium permanganate, and redistilling it from P₂O₅ through a 19-plate bubble-cap Oldershaw column. Tetraethylammonium perchlorate (TEAP) was obtained from G. F. Smith Chemical Co. and dried in vacuo at 60 °C. Lithium trifluoroacetate (Lithium Corp. of America) was dried in vacuo at 100 °C prior to use.

Electrochemical Measurements. Electrochemistry was performed on a Princeton Applied Research Model 173 potentiostat equipped with a Model 176 current-to-voltage converter which provided a feedback com-

pensation for ohmic drop between the working and reference electrodes. The voltage follower amplifier (PAR model 178) was mounted external to the main potentiostat with a minimum length of high-impedance connection to the reference electrode (for low noise pickup). Cyclic voltammograms were recorded on a Houston Series 2000 X-Y recorder. The electrochemical cell was constructed according to the design of Van Duyne and Reilly.⁵² The distance between the platinum working electrode and the tip of the salt bridge was 1 mm to minimize ohmic drop. Bulk coulometry was carried out in a three-compartment cell of conventional design with a platinum gauze electrode. Complete electrolysis of 0.2 mmol of electroactive material generally required 5-10 min and was graphically recorded on a Leeds and Northrup Speedomax strip chart recorder. The current-time curve was manually integrated.

Cyclic Voltammetry. All electrochemical measurements were carried out at 25 °C in acetonitrile solutions with 0.1 M tetraethylammonium perchlorate as the supporting electrolyte. The platinum electrode was routinely cleaned by soaking it in concentrated nitric acid for 15 min followed by repeated rinsing with distilled water and drying at 120 °C prior to use with each alkylmetal. The anodic peak potentials for these alkylmetals were always reproducible to within ± 50 mV, even upon remeasurement after a period of several months. Repeated CV scans did not affect the appearance of the voltammograms, provided the potential was not swept beyond the second anodic wave (which is usually 0.2 to 0.4 V beyond E_p). If the latter occurred, the electrode response subsequently showed a marked deterioration which could only be corrected by recleaning it in nitric acid.

Quantitative Criteria for Total Irreversibility in Cyclic Voltammetry of Alkylmetals. In order to establish that the charge-transfer reaction in the anodic oxidation of alkylmetals is intrinsically slow, i.e., the electrochemical process is totally irreversible, we applied eq 9 and Fick's laws of diffusion to develop the following criteria.

1. Dependence of Peak Potential (E_p and $E_{p/2}$) on Sweep Rate (v). One of the principal tests for electrochemical reversibility rests on the

(46) As discussed in ref 42-44 and critically reviewed in ref 45.
 (47) Nugent, W. A.; Bertini, F.; Kochi, J. K. *J. Am. Chem. Soc.* **1974**, *96*, 4945.
 (48) Tsou, T. T.; Kochi, J. K. *J. Am. Chem. Soc.* **1979**, *101*, 6319.
 (49) Gassman, P. G.; Mullins, M. J.; Richtmeier, S.; Dixon, D. A. *J. Am. Chem. Soc.* **1979**, *101*, 5793.
 (50) (a) Fleischmann, M.; Pletcher, D. *Tetrahedron Lett.* **1968**, 6255. (b) Bertram, J.; Fleischmann, M.; Pletcher, D. *Tetrahedron Lett.* **1971**, 349.
 (51) Mareš, V. M. *Org. React. (NY, Engl. Transl.)* **1967**, *4*, 235; **1968**, *5*, 392, 397.

(52) Van Duyne, R. P.; Reilly, C. N. *Anal. Chem.* **1972**, *44*, 142.

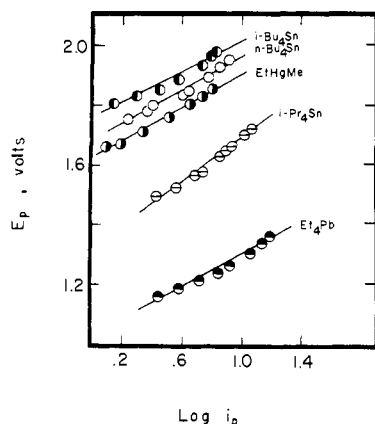


Figure 8. Variation in anodic peak potential E_p with peak current i_p in acetonitrile solutions containing 0.1 M TEAP and the same alkylmetals as in Figure 7.

Table V. Transfer Coefficient Determined by Several Independent Methods^a

alkylmetal	transfer coefficient				
	E_p vs. $\log v$	$E_{p/2}$ vs. $\log v$	E_p vs. $E_{p/2}$	E_p vs. $\log i_p$	av
Me ₄ Sn	0.27	0.35	0.30	0.23	0.29 ± 0.05
Et ₄ Sn	0.33	0.35	0.34	0.29	0.33 ± 0.05
<i>i</i> -Pr ₄ Sn	0.26	0.34	0.30	0.24	0.29 ± 0.05
<i>n</i> -Bu ₄ Sn	0.32	0.36	0.33	0.27	0.32 ± 0.05
<i>i</i> -Bu ₄ Sn	0.30	0.37	0.34	0.26	0.32 ± 0.05
neopentyl ₄ Sn	0.30	0.32	0.31	0.29	0.31 ± 0.05
Et ₄ Pb	0.27	0.36	0.31	0.28	0.31 ± 0.05
EtHgMe	0.28	0.33	0.22	0.24	0.27 ± 0.05

^a See text.

magnitude of the slope in the plot of E_p or $E_{p/2}$ vs. $\log v$.^{20,24,53} Slopes between the limits of 0 and 30 mV per decade are indicative of reversible electron transfer and provide information about the order of the follow-up chemical reactions. In contrast, values greater than 30 mV per decade are predicted for totally irreversible waves on the basis of eq 17.

$$E_p = \frac{2.3RT}{2\beta n_b \mathcal{F}} \log v + \text{constant} \quad (17)$$

(Equation 17 was originally derived by Delahey,³² followed by Nicholson and Shain.²⁰ The same equation has been proposed by Saveant¹⁶ for linear-sweep voltammetry. Except for a different constant term,²⁰ eq 17 also holds for the half-peak potential $E_{p/2}$.) Several representative examples of the dependence of the peak potential on the sweep rate are illustrated in Figure 7. With every alkylmetal studied, the observed slopes of approximately 100 mV per decade are significantly larger than expected for a reversible process. These results provide strong evidence for a totally irreversible electron-transfer process.

2. Constancy of the Transfer Coefficient from Various Properties of the CV Wave. According to eq 17, when the electron-transfer step is totally irreversible, the slope in Figure 8 is given by $2.3RT/2\beta n_b \mathcal{F}$. The transfer coefficients β obtained in this manner are listed in columns 2 and 3 of Table V for E_p and $E_{p/2}$, respectively. The transfer coefficients are consistent with those obtained from other properties related to totally irreversible CV waves, as enumerated in A and B below.

A. The width of the wave in a totally irreversible system has been shown by Nicholson and Shain²⁰ to depend only on the transfer coefficient according to eq 18. The transfer coefficients calculated from this

$$E_p - E_{p/2} = 1.857(RT/\beta n_b \mathcal{F}) \quad (18)$$

equation are listed in column 4 of Table V by using the tabulated values

(53) For some relevant examples see: (a) Saveant, J. M.; Tessier, D. *J. Phys. Chem.* **1978**, *82*, 1723. (b) Andrieux, C. P.; Saveant, J. M. *Electroanal. Chem.* **1971**, *33*, 453. (c) Březina, M.; Koryta, J.; Loučka, T.; Maršiková, D.; Pradač, J. *Ibid.* **1972**, *40*, 13. (d) Gileadi, E.; Stoner, G.; Bockris, J. O'M. *J. Electrochem. Soc.* **1966**, *113*, 586. (e) Lines, R.; Utley, J. H. P. *J. Chem. Soc., Perkin Trans. 2* **1977**, 804. (f) Louis, C.; Benoit, R. L. *Electrochim. Acta* **1973**, *18*, 7. (g) For an alternative derivation of eq 17, see: Matsuda, H.; Ayabe, Y. Z. *Elektrochem.* **1955**, *59*, 494.

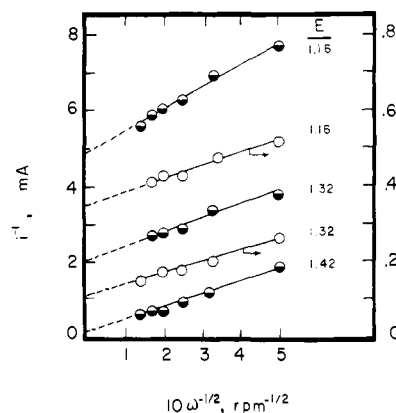


Figure 9. Plot of the current (i_p) vs. rotation rate $(1/\omega)^{1/2}$ of the rotating disk electrode for (●) 9.6×10^{-3} M *i*-Bu₄Sn and (○) 1.3×10^{-2} M Et₄Pb in acetonitrile solutions containing 0.1 M TEAP at 25 °C at the indicated electrode potentials E in V vs. saturated NaCl-SCE.

for the widths of the wave in Table I.

B. The relationship in eq 19 between the peak potential and the peak

$$E_p = \frac{2.3 RT}{\beta n_b \mathcal{F}} \log i_p + \text{constant} \quad (19)$$

current i_p in a totally irreversible wave was first derived by Gokhshtein.⁵⁴ Equation 19 was later rederived by Nicholson and Shain²⁰ with a more accurate value for the constant term. The linearity in the correlation of the peak potential and the peak current ($\log i_p$) is shown in Figure 8 for several representative alkylmetals. The transfer coefficients obtained from the slopes are included in column 5 of Table V.⁵⁵ (Although eq 19 is not completely independent of eq 17 for diffusion-controlled processes, it does provide an internal check on the test for total irreversibility.)

For each alkylmetal, the values of the transfer coefficients obtained by these four methods agree to within the experimental errors. The internal consistency in these values provides additional support for the conclusion that the large slope in the relationship between E_p and $\log v$ in Figure 7 is due to irreversibility of the electron-transfer step.

3. Shape of the CV Wave. Electrochemical waves in which the electron-transfer step is totally irreversible are more elongated along the potential axis compared to those in which the concentration of the electroactive species at the electrode is dictated by the Nernst equation. It is important thus that the transfer coefficients listed in Table V are capable of describing the entire wave. Delahey³² was the first to derive explicit relationships between the potential and current based on the laws of diffusion and the general expression in eq 9 for the rate of electron transfer. Since the form of the equation developed by Nicholson and Shain²⁰ is easier to apply to the general case, we will use it here. In their solution, the current is expressed as a function of time according to eq 20, where $b = \beta n_b \mathcal{F} v / (RT)$ is the normalized sweep rate expressed in

$$i(t) = n\mathcal{F}AC(\pi Db)^{1/2} \chi(bt) \quad (20)$$

units of seconds⁻¹. The function $\chi(bt)$ contains all of the potential dependence, and it has been tabulated by Nicholson and Shain.²⁰ It follows from eq 20 that if both the sweep rate v and the transfer coefficient βn_b are known, the shape of the entire wave can be completely defined. The results of such a calculation based on eq 20 are shown by the circles in Figure 4 at two sweep rates, using the value of the transfer coefficient in Table V for tetraethyltin. (Note that the calculated waves were shifted along the potential and current axes to match the values at the CV peaks, i.e., $t = t_0$ in eq 20 was defined to occur at $E = 1.660$ V.) The excellent agreement between the observed and calculated currents provides compelling evidence that the CV wave can be completely described solely from the rate expression for a totally irreversible charge-transfer step, in conjunction with the laws of diffusion and the transfer coefficients.

Determination of Electrochemical Rates with the Rotated-Disk Electrode. The rotated-disk electrode (RDE) can be used to increase the rate

(54) Gokhshtein, A. Y.; Gokhshtein, V. P. *Dokl. Akad. Nauk SSSR* **1960**, *131*, 601.

(55) The small degree of curvature observed in Figures 7 and 8 has been confirmed by convolutive linear-sweep voltammetry to be due to the potential dependence of the transfer coefficient. A detailed description of this analysis will be presented.³⁸

Table VI. Heterogeneous Rate Constants for the Anodic Oxidation of Alkylmetals. Comparison of the Results from Cyclic Voltammetry and Rotated-Disk Electrode^a

alkylmetal ^b	<i>E</i> , V ^c	log <i>k</i> , cm ⁻¹	
		CV ^d	RDE ^e
Et ₄ Pb	1.555	2.85	2.77
Et ₄ Pb	1.220	2.52	2.32
Et ₄ Pb	1.317	2.04	1.92
<i>s</i> -Bu ₄ Sn	1.155	3.79	3.42
<i>s</i> -Bu ₄ Sn	1.220	3.48	3.33
<i>s</i> -Bu ₄ Sn	1.317	3.00	3.00
<i>s</i> -Bu ₄ Sn	1.417	1.96	2.49

^a In acetonitrile solutions at 25 °C with 0.5 M tetraethylammonium perchlorate as supporting electrolyte. ^b 1.3 × 10⁻² M Et₄Pb and 9.6 × 10⁻³ M *s*-Bu₄Sn. ^c Versus NaCl-SCE. ^d By cyclic voltammetry using eq 11 and data in Tables I, II, and V. ^e By rotated-disk electrode using eq 21.

Table VII. Time Dependence of the Anodic Current for the Oxidation of Tetraisobutyltin^a

time, s	current, μA	<i>i</i> t ^{1/2} , μA s ^{1/2}
0.75	14.3	12.4
1.50	10.4	12.7
2.25	8.3	12.5
3.00	7.1	12.3
3.75	6.3	12.2
4.50	5.7	12.1
5.25	5.4	12.4
6.00	5.0	12.2

^a In acetonitrile solutions at 25 °C with an applied voltage of 1.90 V vs. NaCl-SCE.

of mass transport to the electrode surface. In the limit of infinite rotation rate, the current will be determined only by the rate of electron transfer and given by eq 21,⁵⁶ where ω is the rotation rate, V is the kinematic

$$1/i = 1.61V^{1/6}/(nF D^{2/3} C)\omega^{1/2} + 1/(nF k C) \quad (21)$$

viscosity of the solvent, and the other terms are as described above. Figure 9 is a typical example in which the reciprocal of the current shows a linear dependence on the reciprocal of the square root of the rotation rate. Extrapolation to infinite rotation rate yields the true kinetic current i_k , which is related to the electrochemical rate according to eq 22.⁵⁶ The

$$k(E) = i_k/nFA C \quad (22)$$

area A of the disk was calibrated with a 0.0106 M ferrocene standard (vide infra). The close agreement between the electron-transfer rate obtained in this manner and that obtained from eq 11 by using the CV data is shown in Table VI.

Measurement of the Diffusion Coefficient. The diffusion coefficients in Table II were obtained from analysis of the chronoamperometric $i-t$ transient according to eq 23,^{40b}

$$it^{1/2} = nFA C(D/\pi)^{1/2} \quad (23)$$

In Table VII, the anodic oxidation of tetraisobutyltin is a representative example in which the product of the current and the square root of the time were observed to be constant for periods up to 6 s. The area of the electrode was calibrated with ferrocene in which the diffusion coefficient is $D = 2.4 \times 10^{-5}$ cm² s⁻¹.^{40b}

Double-Step Chronoamperometry of Alkylmetals. A solution of 0.008 M Et₄Sn in acetonitrile containing 0.1 M tetraethylammonium perchlorate was investigated by double-step techniques at 25 °C. The initial voltage (vs. saturated NaCl-SCE) was set at 1.00 V where no current flows. The voltage was then stepped out to +2.00 V (0.20 V more anodic than the cyclic voltammetric peak potential) for a time period (τ), and the resultant anodic current-time data were observed on a Tektronix Model 5115 storage oscilloscope. A sharp charging current spike was observed with a half-life of about 200 μs, followed by a faradic current which decayed as the square root of time. Next the voltage was returned to 1.00 V for an equal time period (τ), and the resultant cathodic current-time data were recorded. The observed cathodic spike was simply

(56) Pleskov, Yu. V.; Filinovski, V. Yu. In "The Rotating Disc Electrode"; Consultants Bureau: New York, 1966; p 91ff.

ELECTRODE POTENTIAL, volts

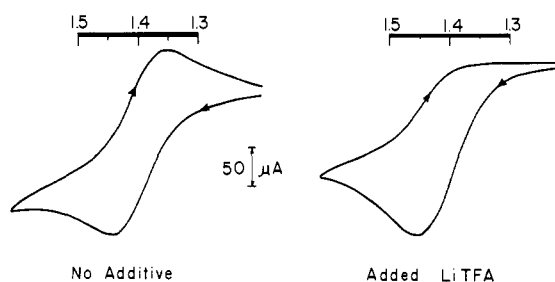


Figure 10. Effect of added nucleophiles on the single-scan cyclic voltammogram of 8.2 × 10⁻⁴ M chromium hexacarbonyl in acetonitrile solutions containing 0.1 M TEAP at a sweep rate of 100 mV s⁻¹. Left: No additives. Right: In the presence of 1.8 × 10⁻³ lithium trifluoroacetate.

equal to that of the charging current (to within the experimental error of ±5%) for time periods as short as 1 ms. The charging currents were measured by performing the same experiment in the absence of alkylmetal. Time periods less than 1 ms could not be used owing to limitations resulting from the charging current. This was determined from the anodic portion of the experiment. Thus at 1 ms, the anodic faradic current is 90% of the observed current but at 500 μs it is only ~5%. This technique¹⁹ thus establishes an upper limit of 1 ms for the lifetime of the alkylmetal cation-radical. A similar conclusion derives from ac polarography of these alkylmetals.

Analysis of Products. Oxidation of Et₄Sn. A solution of 3.03 × 10⁻³ mol of Et₄Sn in 8 mL of acetonitrile containing 0.1 M lithium tetrafluoroborate was exhaustively oxidized at +1.80 V vs. NaCl-SCE. This anodic oxidation required 555 C or 1.90 e for each Et₄Sn. The solvent was removed in vacuo and the resultant solid dissolved in 0.4 mL of CD₃CN to which 5 μL of benzene was added as an internal standard. Integration of the ¹H NMR resonance at δ 1.30 (s) relative to benzene indicated the presence of Et₃Sn⁺ in 99 ± 5% yield. An authentic sample of the cationic moiety Et₃Sn⁺ was prepared from Et₃SnCl and AgClO₄. Addition of a 10-fold excess of LiBF₄ caused no shift in the NMR spectrum of Et₃Sn⁺ClO₄⁻ at δ 1.30 (s) in CD₃CN. Alternatively, Et₃Sn⁺ was analyzed gravimetrically as follows. After exhaustively oxidizing 1.02 × 10⁻⁴ mol of Et₄Sn in 8 mL of acetonitrile containing 0.1 M [Et₄N][PF₆] at +1.80 V, the solvent was removed in vacuo and the resultant solid extracted with four 2-mL portions of ether. The ether was diluted with 20 mL of hexane, and anhydrous ammonia was bubbled through the resultant solution until no further white solid was formed. The precipitate was filtered, washed with hexane, and dried in vacuo in a preweighed fritted glass funnel to yield 20 mg (71%) of Et₃Sn(NH₃)₂⁺PF₆⁻; NMR δ 1.10 (s) relative to sodium (trimethylsilyl)ethanesulfonate in D₂O. Analysis of the gaseous products by gas chromatography (column of Porapak Q) indicated the presence of ethylene (42%) but less than 0.1% ethane, using the internal standard method.

Oxidation of Me₄Sn. A solution of 2.93 × 10⁻⁴ mol of Me₄Sn in 5 mL of CH₃CN containing 0.1 M tetraethylammonium perchlorate was exhaustively oxidized at a potential of +2.50 V at 25 °C. After the solution was diluted with ether, anhydrous ammonia was bubbled through the resultant solution until no further white solid was formed. The precipitate was filtered, washed with hexane, and dried in vacuo in a preweighed fritted glass funnel to yield 80 mg (90%) of Me₃Sn(NH₃)₂⁺ClO₄⁻; NMR δ 0.40 (s) relative to sodium (trimethylsilyl)ethanesulfonate in water.

Oxidation of *t*-BuSnMe₃. A solution of 1.27 × 10⁻⁴ mol of *t*-BuSnMe₃ in 8 mL of acetonitrile containing 0.1 M [Et₄N][PF₆] was exhaustively oxidized at 1.50 V vs. NaCl-SCE. This anodic oxidation required 22.6 C or 1.83 e for each *t*-BuSnMe₃. The solvent was removed in vacuo and the resultant solid extracted with four 2-mL portions of ether. The ether was diluted with hexane, and anhydrous ammonia was bubbled through the resultant solution until no further white solid was formed. The precipitate was filtered into a preweighed fritted glass funnel, washed with hexane, and dried in vacuo to yield 42 mg (90%) of Me₃Sn(NH₃)₂⁺PF₆⁻; NMR δ 0.40 (s) relative to sodium (trimethylsilyl)ethanesulfonate in D₂O. Isobutylene was formed in 13% yield by gas chromatographic analysis (10-ft dibutyl tetrachlorophthalate on Chromosorb P) using the internal standard method. No isobutane was detected.

Dependence of Peak Potential on Following Chemical Reactions—Irreversible and Totally Irreversible EC Processes. The anodic oxidation

(57) Kraus, C. A.; Greer, W. N. *J. Am. Chem. Soc.* **1923**, *45*, 3078.

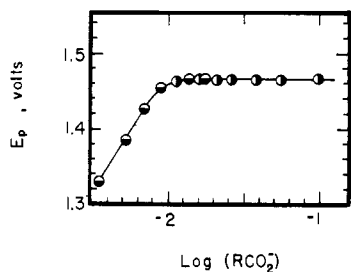
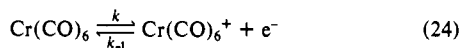


Figure 11. Variation of the anodic peak potential in cyclic voltammetry of $\text{Cr}(\text{CO})_6$ as a function of nucleophile concentrations. (●) $\text{RCO}_2^- =$ acetate and (○) trifluoroacetate as lithium salts. Recorded at a constant sweep rate of 20 mV sec^{-1} . $[\text{Cr}(\text{CO})_6] = 1.0 \times 10^{-3} \text{ M}$ and 0.1 M TEAP .

of $\text{Cr}(\text{CO})_6$ has been shown by cyclic voltammetry to be a reversible one-electron process in acetonitrile solutions²⁷ (see eq 24). However, in



the presence of added nucleophiles such as acetates and trifluoroacetate, the cyclic voltammogram becomes irreversible, owing to the facile anation of the resultant substitution-labile cation in eq 25.⁵⁸ The disappearance



of the reverse cathodic wave, even at low concentrations of lithium trifluoroacetate, is shown in Figure 10. At these low concentrations of nucleophile, the kinetically second-order reaction in eq 8 is sufficiently slow to render the electrochemical process as partially irreversible, as shown by the left side of Figure 11. Under these conditions, the anodic peak potential increases with the rate of the competing anation, in accord with standard electrochemical theory.²⁸ Importantly, above a critical concentration of nucleophile ($\sim 10^{-2} \text{ M}$), the anodic potential is independent of the nature and speed of the following chemical reaction. In other words, when the second-order disappearance of the cation $\text{Cr}(\text{CO})_6^+$ in eq 8 is faster than the reverse rate of electron transfer k_{-1} in eq 7, E_p becomes invariant. Under these conditions the electrochemical wave is considered to be totally irreversible, and the observed peak current i_p is independent of the complexity or the speed of the following chemical reactions.

Acknowledgments. We thank Dr. R. M. Wightman for many helpful discussions, Dr. C. L. Wong for his involvement in the early stages of this work, Dr. D. Peters for the loan of the rotated-disk electrode, and the National Science Foundation for financial support. J. K. Kochi also thanks Dr. R. A. Marcus for helpful discussions and advice.

(58) The facile replacement of carbon monoxide in the cation ion-radicals of metal carbonyls is generally applicable to nucleophiles.⁵ In this study we employed acetate and (at higher concentrations) trifluoroacetate since they yielded the most unambiguous results owing to their electroinactivity at the large positive potentials required to oxidize $\text{Cr}(\text{CO})_6$.

Intramolecular Electron Transfer in the Anion Radicals of Nitrobenzyl Halides¹

P. Neta* and D. Behar

Contribution from the Radiation Laboratory, University of Notre Dame, Notre Dame, Indiana 46556. Received January 21, 1980

Abstract: One-electron reduction of nitrobenzyl halides produces the anion radicals which subsequently undergo intramolecular electron transfer and decompose into nitrobenzyl radicals and halide ions. The optical absorption spectra of the initial anion radicals ($\lambda_{\text{max}} \approx 300\text{--}310 \text{ nm}$) and the subsequently formed nitrobenzyl radicals ($\lambda_{\text{max}} = 350$ and 400 for the para and ortho, respectively) are quite intense ($\epsilon \approx 10^4 \text{ M}^{-1} \text{ cm}^{-1}$ in most cases) and significantly different. This enables identification of the various species and measurement of the rates of intramolecular electron transfer or C–X bond scission. The rates are 4×10^3 , 1.7×10^5 , and $5.7 \times 10^5 \text{ s}^{-1}$ for *p*-nitrobenzyl chloride, bromide, and iodide, respectively. The ortho derivatives decomposed nearly twice as rapidly while the meta decomposed much more slowly. The anion radical of *p*-nitrobenzyl bromide has $\text{p}K_a = 2.8$, and the protonated form is found to undergo the intramolecular transfer ~ 60 times more slowly than the anion radical. The pattern of reactivity of the various anion radicals is rationalized in terms of spin density and charge distribution at the various positions on the ring and in terms of the electrophilicities of the halogens.

Introduction

Intramolecular electron transfer in biopolymers is an important process in many biological redox systems. The transport of an electron through large molecules has been experimentally studied in several systems, including peptides and redox proteins.² Detailed intramolecular electron-transfer mechanisms can be investigated in small model compounds.^{3–5} In several studies

utilizing complexes of Co(III) with aromatic or heterocyclic carboxylic acids an electron transfer from the ligand radical to the central metal ion has been observed.^{3,4} One-electron reduction of (nitrobenzoato)pentamminecobalt(III) complexes was found to produce initially the coordinated nitrobenzoate anion radicals. Subsequently, an intramolecular electron transfer took place from the reduced ligand to the Co(III). The rate constant of this transfer was found to depend strongly on the position of the nitro group relative to the coordinated carboxylate.

In the present work, intramolecular electron transfer within the anion radicals of nitrobenzyl halides is reported. Experiments⁶ have shown that one-electron reduction of nitrobenzyl halides produces initially the anion radicals, which then undergo an intramolecular electron transfer and decompose into halide ions and nitrobenzyl radicals. Such processes have been suggested previously as intermediate steps in several organic substitution reactions.⁷ In this work we report the direct observation of these

(1) The research described herein was supported by the Office of Basic Energy Sciences of the Department of Energy. This is Document No. NDRL-2088 from the Notre Dame Radiation Laboratory.

(2) See, e.g.: Faraggi, M.; Klapper, M. H.; Dorfman, L. M. *J. Phys. Chem.* **1978**, *82*, 508. Pecht, I.; Farver, O.; Goldberg, M. *Adv. Chem. Ser.* **1977**, No. 162, 1979. Simic, M. G.; Taub, I. A. *Faraday Discuss. Chem. Soc.* **1977**, No. 63, 270 and references therein.

(3) Hoffman, M. Z.; Simic, M. *J. Am. Chem. Soc.* **1972**, *94*, 1757. Simic, M. G.; Hoffman, M. Z.; Brezniak, N. V. *Ibid.* **1977**, *99*, 2166.

(4) Cohen, H.; Meyerstein, D. *J. Chem. Soc., Dalton Trans.* **1975**, 2477. Wiegardt, K.; Cohen, H.; Meyerstein, D. *Ber. Bunsenges. Phys. Chem.* **1978**, *82*, 388. Wiegardt, K.; Cohen, H.; Meyerstein, D. *Angew. Chem., Int. Ed. Engl.* **1978**, *17*, 608.

(5) Prütz, W. A.; Land, E. *J. Int. J. Radiat. Biol. Relat. Stud. Phys., Chem. Med.* **1979**, *36*, 513 and references therein.

(6) Preliminary experiments were carried out in this laboratory by V. Madhavan.